Hindawi
Shock and Vibration
Volume 2023, Article ID 5882762, 14 pages
https://doi.org/10.1155/2023/5882762

Research Article

Research on Liquid Flow Rate Detection of Mixed Fluid Based on Vibration Signal Characteristic Analysis of Gas Liquid Two-Phase Flow

Zhang Jian [1] **S. Selvakumar Raja** [2] **Liang Lei** [1] **and Dai Shu** [1]

[1] *Yangtze University, Computer Science, Jingzhou, China*
[2] *University of Gondar, Gonder, Ethiopia*

Correspondence should be addressed to S. Selvakumar Raja; s_selvakumar_raja@126.com

Received 30 December 2022; Revised 25 April 2023; Accepted 5 May 2023; Published 27 June 2023

Academic Editor: Junhong Park

The online detection of liquid flow rate in gas-liquid two-phase flow has become an important factor in ensuring the safe operation of gas wells. In this paper, the real-time measurement of liquid holdup in gas-liquid two-phase flow is carried out by analyzing the characteristics of vibration signals excited by gas-liquid two-phase flow impacting on the pipe wall. Firstly, an acceleration sensing detection and processing system is constructed to obtain the vibration signals excited by gas-liquid two-phase flow impacting on the pipe wall. Then, the pure airflow vibration signals at different flow velocities and the gas-liquid two-phase flow excitation vibration signals at different liquid flow rates are tested, respectively, and the time-frequency characteristics analysis based on STFT is implemented. The practice shows the following: firstly, the frequency band of 6.5–15 Hz is identified as the characteristic frequency band of liquid flow rate in gas-liquid two-phase flow. Secondly, the liquid holdup is positively correlated with the vibration energy in its characteristic frequency band. Thirdly, a mathematical model of the relationship between liquid flow rate and vibration energy is constructed. Finally, the measurement error of liquid holdup is within 10%. This research method has laid a good foundation for the subsequent detection of characteristic parameters of each phase in gas-solid-liquid complex multiphase flow fluids, and it has certain application and promotion value.

1. Introduction

Gas-liquid two-phase flow is a common mixed flow state in the industrial field [1–3], which widely exists in petroleum, metallurgy, firepower, and other industrial production. Due to the interaction between phases and the alternation of time and space, the gas-liquid two-phase flow has the characteristics of complex and changeable flow, violent fluctuation, and strong randomness and presents diversified flow patterns in the pipeline [4–6]. Among them, the flow parameter in the gas-liquid two-phase flow is one of the important parameters to characterize the many characteristics of the gas-liquid two-phase flow. An accurate and efficient flow parameter measurement of gas-liquid two-phase flow is of great significance to improving the safety and stability of gas well production.

Due to the complex and changeable hydrodynamic characteristics of gas-liquid two-phase flow, there are many uncertain factors in its parameter detection [7]. It is difficult to achieve an accurate measurement of the two-phase flow characteristic parameters, especially the flow rate of mixed fluid, only by means of the traditional single-phase flow parameter measurement method. Accurate detection of liquid holdup in multiphase flow has become a hot research issue in this field [8]. The research on its online detection method is of great significance for the production management, control, and safe operation and maintenance of oilfield gas well production operations.

In recent years, researchers have carried out continuous research on the detection methods of flow parameters in gas-liquid two-phase flow. Based on the Doppler shift information obtained by UVP, Wang used the ultrasonic pulse echo intensity information to judge the phase interface so as to measure the flow rate of oil-gas-waterthree-phase stratified flow and compare it with the results of PIV and a high-speed camera [9]. Murdock gave a modified calculation formula for the split-phase flow model by performing a gas-water mixture experiment [10]. Chisholm assumed that the gas-liquid two-phase flow through the orifice plate is a split-phase flow, and the measurement model of the orifice plate split-phase flow is derived from the gas-liquid two-phase flow equation [11]. Xu et al. from Tianjin University used a double differential pressure long throat Venturi flow sensor as a measurement method to predict the gas-liquid two-phase flow of wet gas through computational fluid dynamics simulation technology [12]. Li put forward the design idea of installing the near-infrared probe along the direction of fluid flow and proved the advantages of the new gas-liquid two-phase flow detection device in using near-infrared to measure phase holdup through experiments [13]. Fang used laser diode with a wavelength of 980 nm and silicon photodiode to carry out real-time online measurements of gas-liquid two-phase flow in horizontal and vertical directions [14]. Liang determined the wavelength of near-infrared light through static and dynamic experiments and obtained the estimated value fitting formula of phase content [15]. By analyzing the relationship between the propagation velocity, temperature, and medium density of an ultrasonic wave in light fuel, Zhang et al. established a model by using artificial neural network and completed the mass flow measurement of light fuel [16]. Hou et al. established the functional relationship between energy fraction and particle size by using the vibration noise signals collected by acoustic emission with different particle size distributions from the collision between particles in a gas-solid fluidized bed and distribution plate [17].

The abovementioned detection methods have played a positive role in promoting the development of gas-liquid two-phase flow measurement methods, but there are few reports on the monitoring of liquid flow rate in gas-liquid two-phase flow. At the same time, the time-frequency analysis of unsteady and nonlinear random signals excited by gas-liquid two-phase flow impacting on the pipe wall has not achieved a unified and complete description. Ong et al. constructed a threshold function based on wavelet transform to characterize the noise excited by the fluid, but it is difficult to construct a wavelet base matching the fluid's characteristics [18]. Aghdam et al. extracted the features of nonstationary vibration signals based on the ARMA time series model, but there are some problems such as complex modeling, contradiction between order selection, and calculation amount [19]. Liu obtained the optimal time-frequency representation of energy concentration based on the VWD distribution, but it is disturbed by the cross terms when analyzing the multicomponent signals [20]. In summary, it is of great practical significance to study the detection method of liquid flow rate in gas-liquid two-phase flow based on the analysis of time-frequency characteristics of vibration signals.

Aiming at the problem of liquid production in gas wells at high water cut stage, an innovative method is designed in this paper, which uses an acceleration sensor detection system to obtain the vibration signals excited by fluid impact at the elbow pipe wall and analyzes the time-frequency characteristics of the signal to monitor the change in the liquid flow rate. Compared with traditional detection methods, this method has the advantages of convenient installation, real-time online monitoring, better accuracy, and higher cost performance. At the same time, this method can also provide technical support for adjusting the production parameters in time, reducing excessive liquid production, improving gas well recovery efficiency, reducing costs, and increasing the efficiency of gas production.

2. Characteristic Analysis of Vibration Signals Excited by Liquid Particle in Gas-Liquid Two-Phase Flow

The gas-liquid two-phase flow has a certain kinetic energy when flowing in the pipeline. When the gas-liquid mixed fluid passes through the 90° elbow of the pipeline at a higher speed, due to the sudden change of the flow direction, the liquid particles will break away from the drag force of the air flow under the inertial action and impact the pipe wall and cause vibration, as shown in Figure 1.

The liquid particles in the gas-liquid two-phase flow impact the pipe wall to generate continuous kinetic energy. The acceleration sensor arranged outside the elbow picks up the vibration signal and further converts it into the required liquid particle parameters. The kinetic energy KE excited by the liquid particle impact is shown in the following formula:

$$\mathrm{KE} = \frac{1}{2}\mathrm{mv}^2. \tag{1}$$

In the formula, m is the mass of liquid particles and v is the velocity of liquid particles impacting on the pipe wall. It can be concluded from the qualitative analysis that the kinetic energy of liquid particles is positively correlated with its mass, and the kinetic energy of liquid particles increases exponentially with its migration velocity.

The nonstationary and nonlinear random vibration signals excited by the low content liquid droplet impacting on the pipe wall in the gas-liquid mixed flow are very weak, and the conventional signal processing methods are based on static assumptions. Therefore, only the statistical characteristics of the signals are studied in a single range of time domain or frequency domain, which cannot reveal the independent characteristics of the liquid particle signals in the time-frequency joint domain. In order to effectively distinguish the different characteristics of the signals excited by the liquid particle impacting on the pipe wall and the air flow impacting on the pipe wall [21] and at the same time make up for the deficiency that the conventional Fourier transform method cannot be applied to the analysis of nonperiodic and nonstationary signals [22], in this paper, the time-frequency analysis method based on the short-time Fourier transform (STFT) [23] is adopted to process the

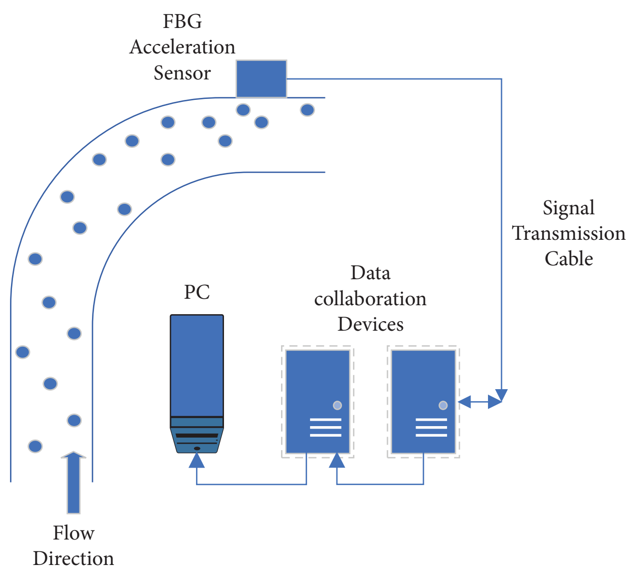

Figure 1: Monitoring diagram of vibration induced by liquid particles impacting the pipe wall in gas-liquid two-phase flow.

random signal excited by the liquid particle impacting on the pipe wall. Yichen Li et al. [24] proposed a method for monitoring sand production in offshore oil wells which are based on the vibration response characteristics of sand-carrying fluid flow impinging on the pipe wall. This method uses acceleration sensors to obtain the weak vibration response characteristics of sand particles impinging on the pipe wall on a two-dimensional time-frequency plane. The time-frequency parameters are further optimized, and the ability to identify weakly excited vibration signals of sand particles in the fluid stream is enhanced. In this method, the window function method operation is first performed on the nonstationary signal, and the signal is segmented at a series of short-time intervals, which is similar to the superposition of several stationary signals. Once again, the Fourier decomposition operation is carried out for each approximated stationary signal. The short-time Fourier transform method not only solves the defect that the traditional Fourier transform cannot reflect the time resolution but also solves the frequency aliasing problem that the conventional wavelet transform cannot avoid in the frequency domain. It can directly provide the broad-spectrum frequency characteristics of the signals and the corresponding energy characteristics, and the energy amplitude is characterized as follows:

$$\mathrm{TF}(t,f)=\left|\int_{-T}^{T} y(\tau)h*\left|(\tau-t)e^{-i2\pi f\tau}\mathrm{d}\tau\right|.\right. \quad (2)$$

In the formula, $h*(\tau-t)$ is a window function centered on $t=0$, which has time aggregation and frequency aggregation. Its transformation can be regarded as the decomposition of the signal on the orthogonal basis function. The basis function has both time and frequency resolution in different transformations.

After obtaining the characteristic frequency band of the vibration signals excited by the liquid particle impact, band-pass filtering is used to further filter out the characteristic signal of the airflow frequency band, and then the fluid particle frequency band signal is extracted. The transfer function is as follows:

$$H(z)=\frac{\sum_{0}^{M} a_{1k} z^{-k}}{1+\sum_{k=1}^{N} b_{1k} z^{-k}}. \quad (3)$$

In the formula, N is the filtering order, M is the zero point of the transfer function, and a_{1k} and b_{1k} are weight function coefficients.

The power spectrum characteristics of the random vibration signals excited by the multiphase flow impacting on the pipe wall reflect the variation characteristics of the signal power with frequency in the unit frequency band. Therefore, the variation law of the random signal energy with frequency can be obtained by the power spectrum density function. The average power of the power spectrum signal $f(t)$ in the time domain $t=[-(T/2),(T/2)]$ can be expressed as follows:

$$P=\lim\frac{1}{T}\int_{-(T/2)}^{(T/2)} f^{2}(t)\mathrm{d}t = \frac{1}{2\pi}\int_{-(T/2)}^{(T/2)} \lim\frac{\left|F_T(\omega)\right|^{2}}{T}\mathrm{d}\omega. \quad (4)$$

3. Experimental Design and Signal Detection Method Research

3.1. Experimental Device. The two-phase mediums in the gas-liquid two-phase flow rate test are air and water. Figure 2 is composed of gas supply system, liquid supply system, test pipe section, metering system, signal acquisition system, and gas-liquid separation system [25].

In the liquid supply system, the tap water extracts the water from the liquid metering tank into the single-phase pipe section of the water flow. The opening of the tap water valve can adjust the size of the water flow. The liquid metering tank (with the measurement range of 0–20 m^3/h, flow velocity range of 0–2.83 m/s, and accuracy of ±0.5%) is used to measure water flow before mixing.

In the gas supply system, the air is pressurized by the air compressor (the maximum displacement is 35 m^3/min) and sent to the gas tank, and then the compressed gas is fully dried by the air dryer. The tape gas valve is installed between the gas tank and the blender. The regulating valve can play the role of depressurization and pressure stabilization to ensure the stability of the gas tape pressure during the experiment. At the same time, the opening of the tape gas valve is controlled to adjust the intake gas flow rate. The gas metering tank (with the measurement range of 0–210 m^3/h and accuracy of ±1%) measures the gas flow rate before mixing.

The inner diameter of the test pipe is 60 mm, and the whole pipe section is about 14 m. The length of the pipe involved in the experiment is 9.5 m, and the observation section is a transparent organic glass pipe of 7 m, so as to observe the liquid carrying state of the airflow and the gas-

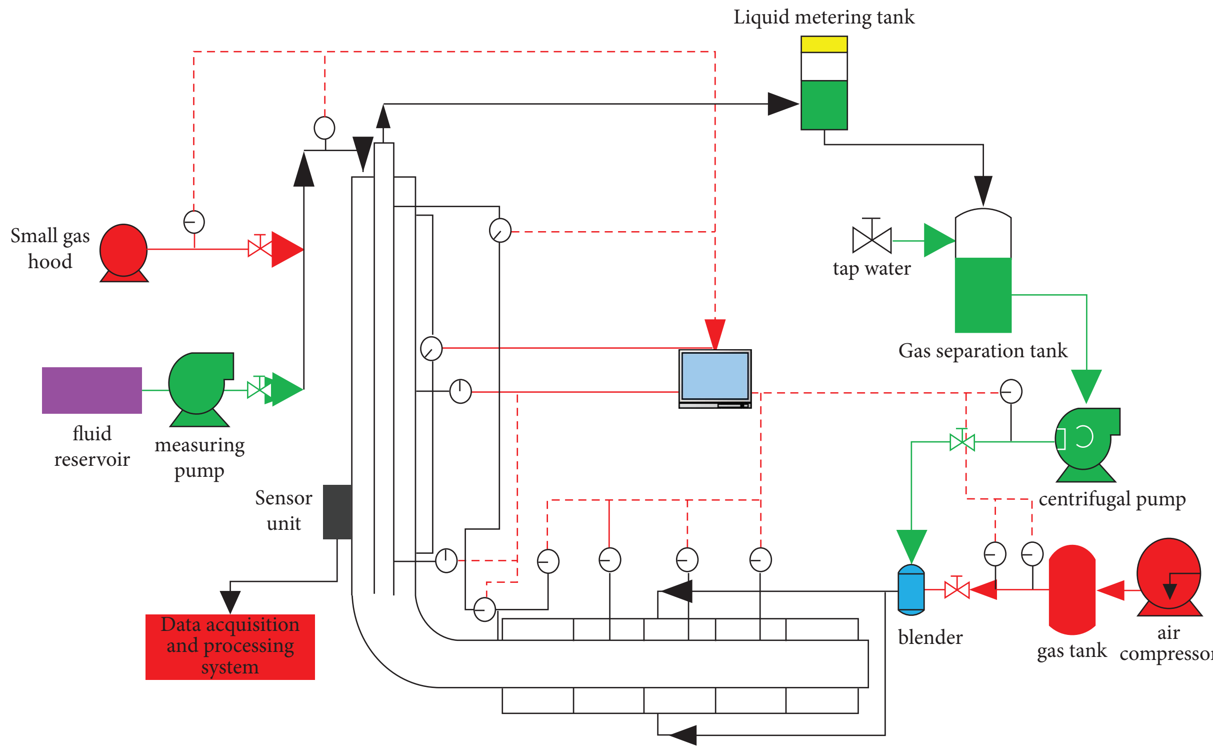

Figure 2: Structure diagram of experimental device.

liquid two-phase flow pattern. The inlet and outlet of the test pipe are respectively provided with quick closing valves. The distance between the two quick closing valves is 9.5 m.

The air and water excited by the pump and the air compressor respectively enter from two pipe branches, as shown in Figure 3. When starting the experimental device, the liquid is first filled with the pipeline, and the pneumatic valve is opened after the water flow velocity is stable, and then the gas flow rate is adjusted from small to large. Gas-liquid two phases respectively flow in their single-phase pipes for a certain distance and then reach a stable flow velocity. The flow velocity is measured by a standard flowmeter, and then gas-liquid two phases are fully mixed by a jet and sent to the horizontal test pipe section for experiment. The high-speed camera is used to photograph the two-phase flow pattern in the pipe.

Acceleration sensors are arranged at 2-3 times the pipe diameter of the lower elbow of the pipeline, that is, the position where the liquid particles impact the pipe wall at a high speed to obtain the vibration signals excited by the pure airflow and the gas-liquid two-phase flow impacting on the pipe wall. The vibration signals excited by the simulated gas well liquid production under indoor experimental conditions are obtained through the acceleration sensor and data processing system.

3.2. Experimental Design. The experimental parameters for characteristic analysis of gas-liquid two-phase pipe flow excitation signal are shown in Table 1, and the experimental process is as follows:

(1) Experimental temperature is 24°C. The gas volume regulation increases from 10, 20, 30, 40, 50, and 60 m^3/h in turn, and the step is 10 m^3/h. Liquid volume regulation increases from 0.2 to 0.6 m^3 as needed.

(2) After the gas-liquid mixing is carried out on the experimental platform, the gas-liquid two-phase flow through the 90° elbow pipe causes the liquid particles impacting on the pipe wall, so as to stimulate the vibration signal. A total of 18 sets of tests are carried out after the combination of the gas and liquid at different flow rates.

(3) Due to the hardware limitations of the experimental device and the change in the measurement method, the values of the parameters in the table are within the error range.

4. Flow Characteristics of Gas-Liquid Two-Phase Flow

The flow pattern of two-phase flow near the pipe elbow is studied by using the conventional observation method [26]. In order to obtain the vibration signals excited by liquid particles impacting on the pipe wall in gas-liquid two-phase flow as comprehensively as possible, the flow velocity interval that is relatively stable in a specific range and has no obvious change in the trajectory observation is selected as the observation object.

By observing the flow characteristics of gas-liquid two-phase flow in the flow velocity range of 0.46–1.2 m/s, the

Figure 3: Physical drawing of gas and liquid branch pipelines.

trajectory of the liquid is characterized by the movement trend of the fluid. The flow direction and trajectory of the bubble in the pipe flow are relatively stable, and the trajectory line gradually becomes longer as the flow velocity increases. Under this experimental condition, the motion characteristics of the fluid do not change significantly. Therefore, the flow velocity range of 0.46–1.2 m/s can be used as the basic parameter for the liquid phase detection of fluid flow in gas-liquid two-phase flow.

The application range of this measurement method is suitable for the measurement scenario combining medium gas flow range (0–60 m^3/h) and small flow range (0.2–0.6 m^3/h). In such a mixing mode of medium gas volume and small liquid volume, the gas-liquid mixed fluid presents a liquid bubble flow, in which the liquid presents a liquid particle state under the impact of the gas flow, which is suspended in a large amount of gas and moves forward at a constant speed, impacting the pipe wall at the elbow and causing vibration.

5. Analysis of Experimental Results

In this paper, the three-dimensional spectral array diagram analysis method based on STFT is used to analyze and study the nonstationary and nonlinear random vibration signals of gas-liquid two-phase flow. The spectrum array diagram superimposes the energy of the vibration signal with time into a three-dimensional spectrum diagram, showing the relationship between the frequency and amplitude of the signal with time. The logarithmic coordinate is selected for the energy amplitude. The basic principle is as follows:

$$\mathrm{STFT}_S^{(\gamma)}(t, f) = \int_{-T}^{T} [x(\tau)\gamma^*(\tau - t)] \exp(-j2\pi f \tau) \mathrm{d}t, \quad (5)$$

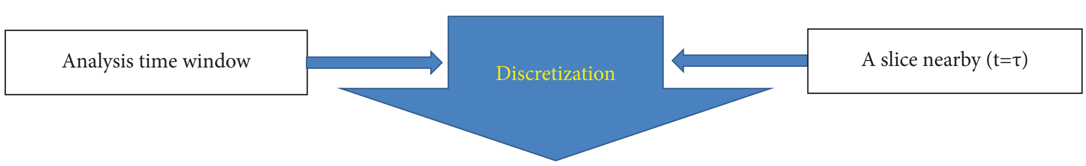

$$\mathrm{STFT}(n, k) = \sum_{i=0}^{N-1} x(i)\gamma^*(i - n)] \exp\left(-j\frac{2\pi k i}{N}\right). \quad (6)$$

5.1. Time-Frequency Characteristic Analysis of Airflow Signal at Different Flow Velocities. The vibration signals excited by the gas-liquid two-phase flow impacting on the pipe wall are the superposition of the strong vibration signals excited by airflow impacting on the pipe wall and the weak vibration signals excited by liquid particles impacting on the pipe wall. Figure 4 shows the time domain characteristics of the vibration signals excited by the airflow impacting on the pipe wall at different flow velocities. The amplitude of the time domain signal is positively correlated with the change in the airflow velocity, so the flow velocity has a great influence on the signal amplitude. In order to effectively extract the weak vibration signals excited by the liquid particle impacting on the pipe wall in the gas-liquid two-phase flow, it is necessary to further analyze the characteristics of the relatively strong vibration signals excited by the airflow impacting on the pipe wall.

Figure 5 shows the frequency domain characteristics of airflow signals at different flow velocities. The results show that the amplitude of the signal changes significantly with the flow velocity in the frequency band range of 45–75 Hz. This frequency band is identified as the main frequency band of the vibration signals excited by the airflow impacting on the pipe wall, indicating that the flow velocity has a significant impact on the signal in this frequency band. Therefore, it is not suitable to find the signal characteristics of liquid particles in this frequency band.

Table 1: Experimental measurement parameters for characteristic analysis of gas-liquid two-phase pipe flow excitation signals.

Gas flow rate (m^3/h)	Liquid flow rate (m^3/h)	Fluid velocity (m/s)	Pressure (Kpa)	Pressure difference (Kpa)	Measurement point
8.7	0.22	0.21	5.02	−1.30	
19.63	0.22	0.46	5.31	−2.03	
32.12	0.22	0.75	6.63	−4.49	
38.49	0.22	0.90	7.59	−6.12	
51.3	0.21	1.20	8.6	−8.90	
59.88	0.21	1.39	14.19	−20.28	
11.31	0.33	0.27	4.45	1.58	
19.35	0.33	0.46	6.61	−3.63	
30.23	0.33	0.71	5.96	−1.56	Acceleration sensor unit (at 2-3 times the pipe diameter of the lower elbow of the pipeline)
38.40	0.33	0.89	7.31	−4.68	
49.8	0.33	1.16	11.45	−13.26	
58.76	0.33	1.40	19.56	−11.49	
9.80	0.61	0.24	9.21	1.94	
20.06	0.61	0.48	12.64	5.42	
29.66	0.61	0.70	16.13	3.43	
40.07	0.61	0.94	24.04	2.08	
51.17	0.61	1.20	39.64	2.33	
61.03	0.61	1.43	71.56	−10.21	

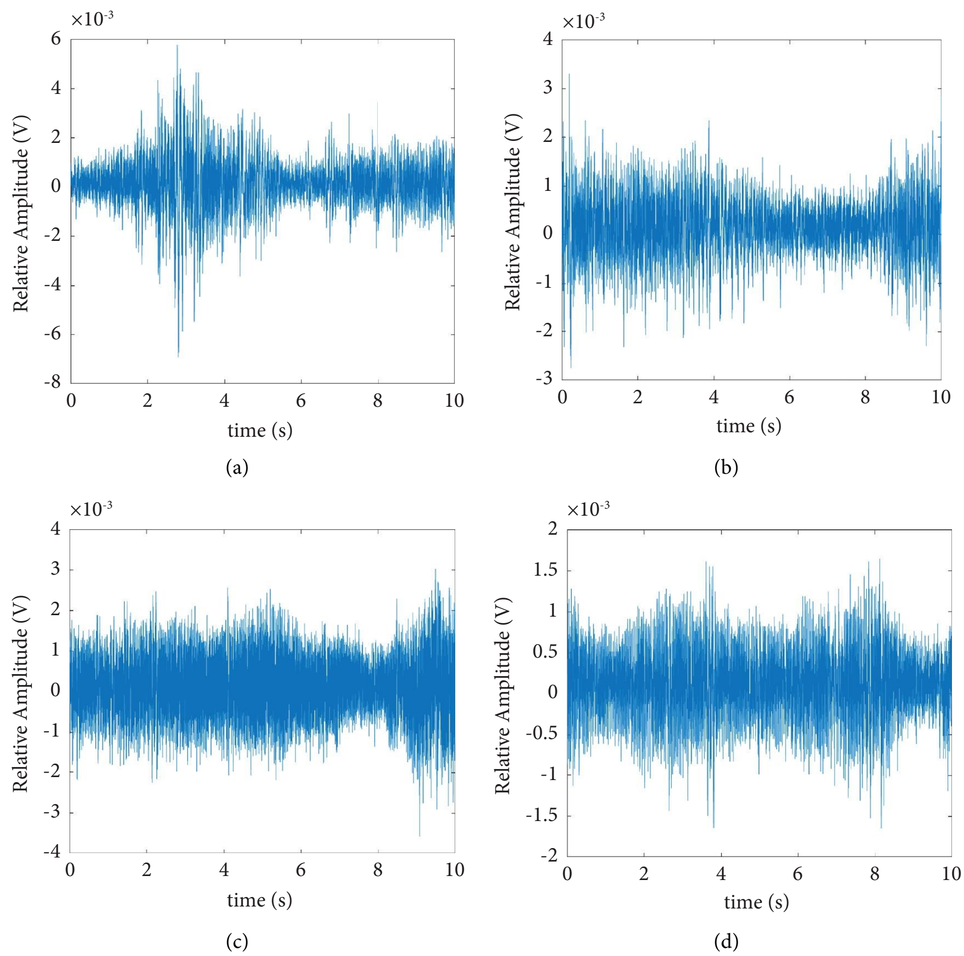

Figure 4: Time domain characteristics of airflow signals at different flow velocities. (a) 0.46 m/s. (b) 0.75 m/s. (c) 0.89 m/s. (d) 1.20 m/s.

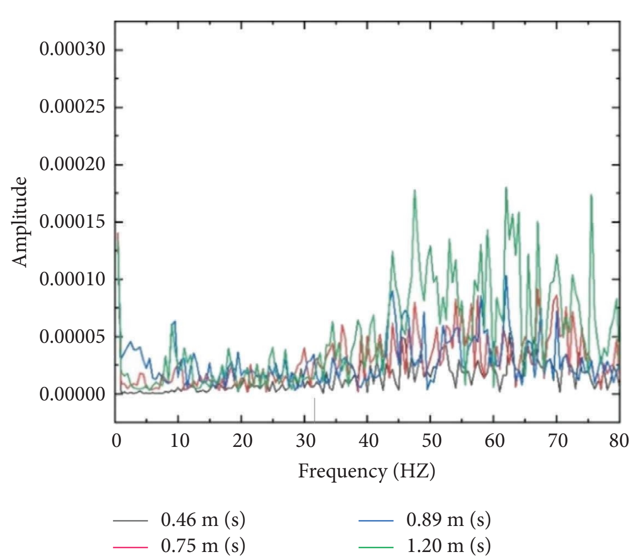

Figure 5: Frequency domain analysis results of pure airflow signals at different flow velocities.

The gas-liquid two-phase flow impacts the elbow pipe wall to generate nonstationary and nonlinear random vibration signals. However, the traditional Fourier transform analysis only reveals the statistical characteristics of the signals in the frequency domain and cannot express the time-varying characteristics of the airflow signals in the joint time-frequency plane. Therefore, the STFT time-frequency analysis method is selected to further study the time-varying energy characteristics of the vibration signals excited by the airflow impacting on the elbow pipe wall at different flow velocities. Figure 6 shows the 3D surface diagram analysis of the vibration signals excited by the airflow impact at different flow velocities in a certain period of time. The selected window function is Hamming window [27], and the FFT length is 20000 points.

It can be seen from Figure 6(a) that when the flow velocity is 0.46 m/s, the frequency domain range of the signal excited by the airflow impact is concentrated in the three frequency bands of 6.5–15 Hz, 34–43.5 Hz, and 45–78.5 Hz. In the range of 45–78.5 Hz, the signal intensity is higher than that in other frequency bands, and the stability is acceptable. In the range of 34–43.5 Hz, the signal strength and the stability take the second place. In the range of 6.5–15 Hz, the signal intensity is relatively low, and the signal amplitude fluctuation is weak. In summary, at a flow velocity of 0.46 m/s, the characteristic frequency band of the signal excited by the airflow impacting on the pipe wall is determined to be within the range of 45–78.5 Hz.

By analyzing the results of Figures 6(b)–6(d), it is concluded that the frequency response characteristics of the vibration signals excited by the airflow impacting on the pipe wall are roughly similar to those of Figure 6(a) when the fluid velocities are 0.75 m/s, 0.89 m/s, and 1.20 m/s, respectively.

5.2. Analysis of Time-Frequency Characteristics of Vibration Signals Excited by Gas-Liquid Two-Phase Flow at Different Flow Velocities. Due to the small particle size of the liquid particles in the gas-liquid mixed fluid, the flow velocity of the liquid particles in the pipeline can be regarded as similar to the flow velocity of the gas in the pipeline. The time domain and frequency domain analysis of gas-liquid mixed fluid at different flow velocities is carried out. The results are shown in Figures 7 and 8.

It can be seen from Figure 8 that in the frequency band of 45–78.5 Hz, the range and trend of signal amplitude show significant change in characteristics with the change in flow velocity. Compared with the time domain analysis results in Figure 7, at different flow velocities, the amplitude change of signal in the same frequency band of 45–78.5 Hz is very similar to the trend change, so this frequency band is considered as the sensitive frequency band of the two-phase flow. However, the frequency band for analyzing the characteristics of vibration signals excited by the liquid particles impacting on the pipe wall should be within 5–15 Hz, and the amplitude of the signal frequency domain shows a small order of fluctuation characteristics. Therefore, this frequency band is selected as the characteristic frequency band of the vibration signals excited by the liquid particle impacting on the pipe wall.

The STFT time-frequency analysis method is used to analyze the characteristics of the vibration signals excited by the gas-liquid two-phase flow impacting on the elbow pipe wall. Figure 9 shows the 3D surface energy analysis results of the vibration signals excited by the gas-liquid two-phase flow within a certain time range.

As can be seen from Figure 9(a), when the gas-liquid two-phase flow velocity is 0.46 m/s, the frequency range of the excited vibration signals mainly focuses on the three frequency bands of 40–75 Hz, 34–43.5 Hz, and 6.5–15 Hz. The signal amplitude intensity in the frequency band of 34–43.5 Hz is lower than before; at the same time, the signal stability is also reduced. The signal amplitude intensity in the frequency band of 6.5–15 Hz is higher than that in the frequency band of 34–43.5 Hz, but the fluctuation of signal amplitude is obvious. Therefore, when the airflow velocity is 0.46 m/s, the main frequency band of the signal excited by the gas-liquid two-phase flow impacting on the pipe wall is 40–75 Hz, and the frequency band with obvious fluctuation is 6.5–15 Hz.

The analysis results of Figures 9(b)–9(d) show that when the fluid velocities are 0.75 m/s, 0.89 m/s, and 1.20 m/s, respectively, the frequency response characteristics of the signals excited by the gas-liquid two-phase flow impacting on the pipe wall are consistent with Figure 9(a).

By comparing the analysis result of the spectral array diagram of vibration signals excited by airflow in Figure 6 with that of vibration signals excited by gas-liquid two-phase flow in Figure 9, it is concluded that the frequency band of vibration signals excited by two-phase flow impacting on the pipe wall is mainly concentrated in 40–75 Hz, but the signal amplitude fluctuates significantly in the range of 6.5–15 Hz. Therefore, the signal excited by the liquid particles impacting on the pipe wall in the 40–75 Hz frequency band is easily submerged, and then the 6.5–15 Hz frequency band is identified as the characteristic frequency band of the vibration signals excited by the liquid particles impacting on the pipe wall.

5.3. Relationship between Liquid Content and Vibration Energy in Gas-Liquid Two-Phase Flow. The feasibility of the vibration signal detection method in this paper is verified by constructing a mathematical model of liquid flow rate in gas-liquid two-phase flow. The vibration energy excited by gas-liquid two-phase flow impacting on the pipe wall is expressed by E_V, as follows:

$$E_V = \frac{1}{T}\int_0^T V^2(t)\mathrm{d}t. \tag{7}$$

In the formula, $V(t)$ is the voltage value obtained after signal processing and T is the sampling time length of the signal. The signal refreshing period is 0.5 s and the sampling length is 20,000 points.

In order to reduce the influence of airflow noise on the characteristics identification of vibration signals excited by liquid particles impacting on the pipe wall, the energy characteristics of them are further studied. By comparing the

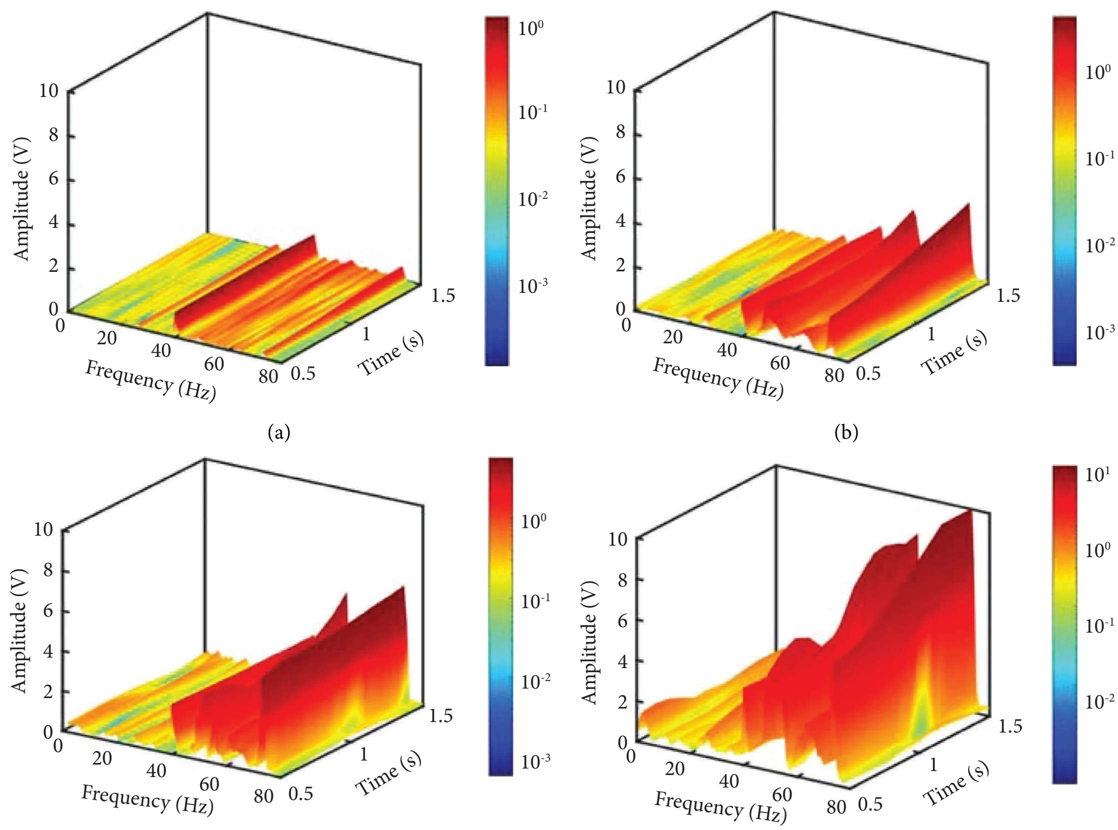

Figure 6: Spectral array diagram of airflow at different flow velocities. (a) 0.46 m/s. (b) 0.75 m/s. (c) 0.89 m/s. (d) 1.20 m/s.

frequency domain characteristics of the vibration signals excited by the gas flow and gas-liquid two-phase flow impacting on the pipe wall at different flow velocities, band-pass filtering is carried out on the frequency band of the signals excited by the liquid particles impacting on the pipe wall in the range of 6.5–15 Hz. Figure 10 shows the relative average vibration energy of the signals excited by the liquid particles impacting on the pipe wall at different liquid flow rates and flow velocities. The velocities of liquid particles impacting on the pipe wall are 0.46 m/s, 0.75 m/s, 0.89 m/s, and 1.2 m/s, respectively. The results show that with the increase in the liquid flow rate and two-phase flow velocity, the vibration energy excited by liquid particles impacting on the pipe wall is positively correlated with it.

The third-order polynomial is used to fit the relative average vibration energy of the flow velocity in the range of 0.46 m/s–1.20 m/s, and the relationship between the velocity of the liquid impacting on the elbow pipe wall and the relative average vibration energy is obtained. $F(v, f)_{\text{liquid}}$ is recorded as the relative average vibration energy excited by liquid particles impacting on the pipe wall in the gas-liquid two-phase flow, where v is the flow velocity and f is the signal bandwidth. The expression after a polynomial fitting is as follows:

$$F(v, f)_{\text{liquid}} = a_0 + a_1 v + a_2 v^2 + a_3 v^3. \quad (8)$$

The signals in the liquid content characteristic frequency band of 6.5–15 Hz in the gas-liquid two-phase flow are preprocessed to obtain the relative average vibration energy of the vibration signals excited by gas-liquid two-phase flow impacting on the pipe wall under different conditions. Figure 11 shows the distribution of relative average vibration energy excited by gas-liquid two-phase flow impacting on the elbow pipe wall under different liquid flow rates and flow velocities.

As shown in Figure 11, when the liquid flow rate is constant, the relative average vibration energy excited by gas-liquid two-phase flow impacting on the pipe wall shows a positive correlation with the increase in two-phase flow velocity. When the flow velocity is constant, the relative average vibration energy excited by gas-liquid two-phase flow impacting on the pipe wall is positively correlated with the increase in liquid flow rate. Third-order polynomial is used to describe the vibration signals excited by liquid flow impacting on the pipe wall at different flow velocities, as shown in the following formula:

$$G_{\text{liquid}}(v) = b_0 + b_1 v + b_2 v^2 + b_3 v^3. \quad (9)$$

When the liquid flow rate is set to zero, the average vibration energy corresponding to different flow velocities is substituted into formula (9), and the fitting coefficient of third-order polynomial is obtained as shown in Table 2.

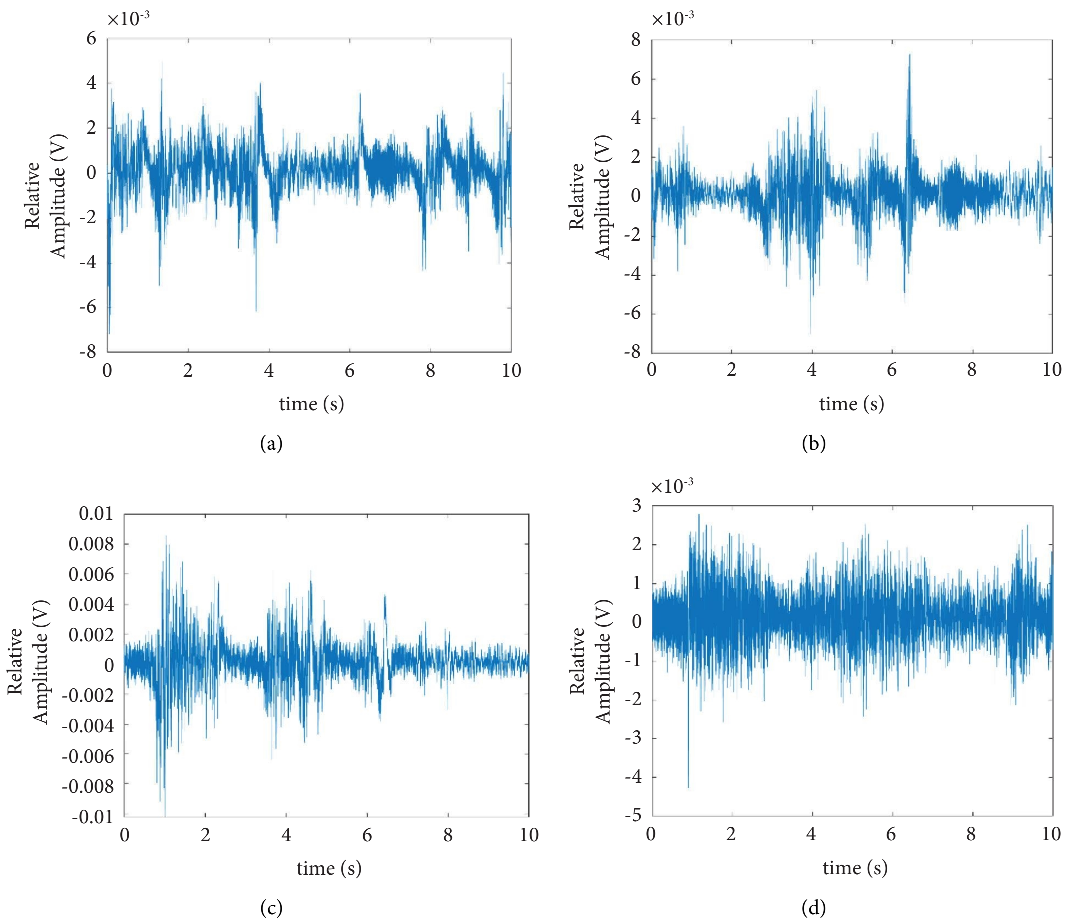

Figure 7: Time domain analysis of vibration signals excited by gas-liquid two-phase flow at different flow velocities. (a) 0.46 m/s. (b) 0.75 m/s. (c) 0.89 m/s. (d) 1.20 m/s.

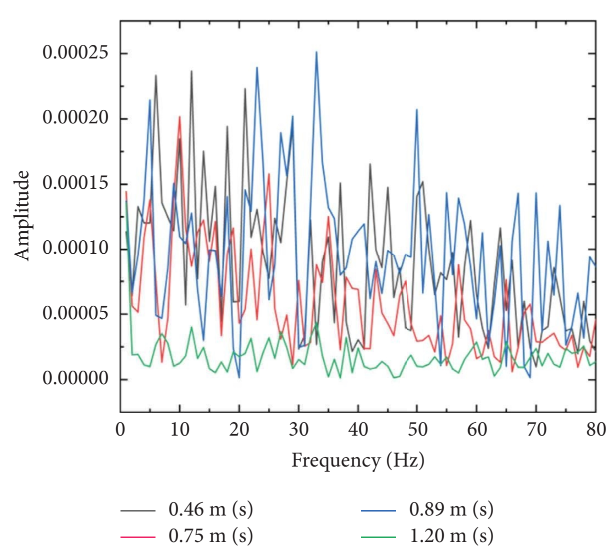

Figure 8: Frequency domain analysis of vibration signals excited by gas-liquid two-phase flow at different flow velocities.

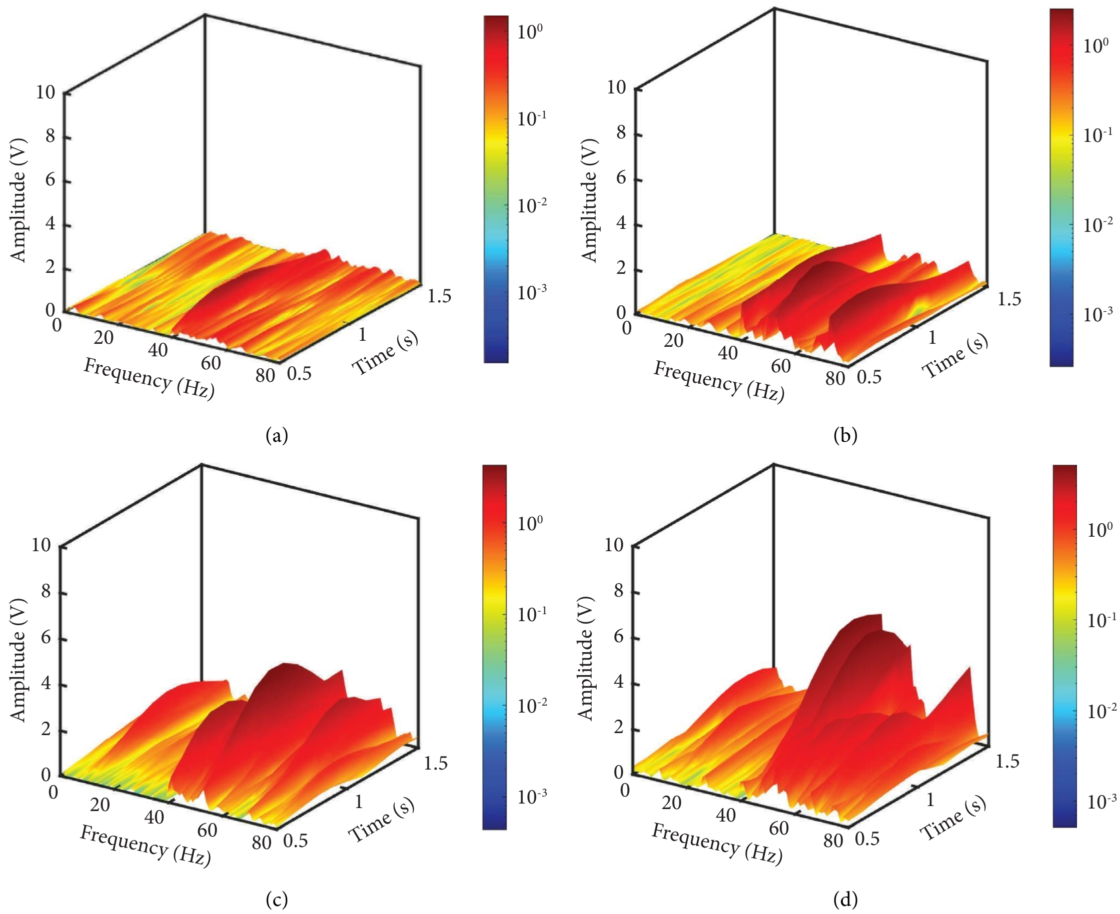

Figure 9: 3D surface spectral array diagram of vibration signals excited by gas-liquid two-phase flow at different flow velocities. (a) 0.46 m/s. (b) 0.75 m/s. (c) 0.89 m/s. (d) 1.20 m/s.

The vibration signals excited by gas-liquid two-phase flow impacting on the elbow pipe wall are processed and converted into corresponding vibration energy, which can describe the change trend of liquid flow rate. However, in order to obtain more accurate liquid flow rate, it is necessary to preprocess the vibration signal energy, that is, the amplitude of vibration signals excited by gas-liquid two-phase flow impacting on the pipe wall subtracts the amplitude of vibration signals excited by pure airflow impacting on the pipe wall under the same condition. The preprocessed vibration signals excited by gas-liquid two-phase flow impacting on the pipe wall divides by the calibration vibration signals excited by the liquid flow impacting on the pipe wall to obtain a relatively accurate liquid flow rate by using the quantitative analysis. Referring to the calibration liquid flow signal, that is, the vibration signals excited by liquid particle impacting on the pipe wall under the condition of 1 m/s liquid flow, the calculation method of the liquid flow rate is as follows:

$$\begin{aligned}\text{liquid flowrate} &= \frac{E_{v,\text{gas-liquid}} - G_{\text{gas}}(v)}{F(v,p)|_{(1m/s,f)}} \\ &= A\frac{(1/T)\int_0^T V^2(t)\mathrm{d}t - \left(b_0 + b_1 v + b_2 v^2 + b_3 v^3\right)}{a_0 + a_1 v + a_2 v^2 + a_3 v^3}.\end{aligned} \tag{10}$$

The vibration signals excited by gas-liquid two-phase flow impacting on the pipe wall at different flow velocities are calculated by formula (10) to verify the accuracy of the liquid holdup calculation formula. Three experiments are carried out at each flow velocity, as shown in Figure 12. The triangle marks in the figure show the liquid flow rate calculated by formula (10). As shown in the figure, the calculated value fluctuates within 10% of the normal error

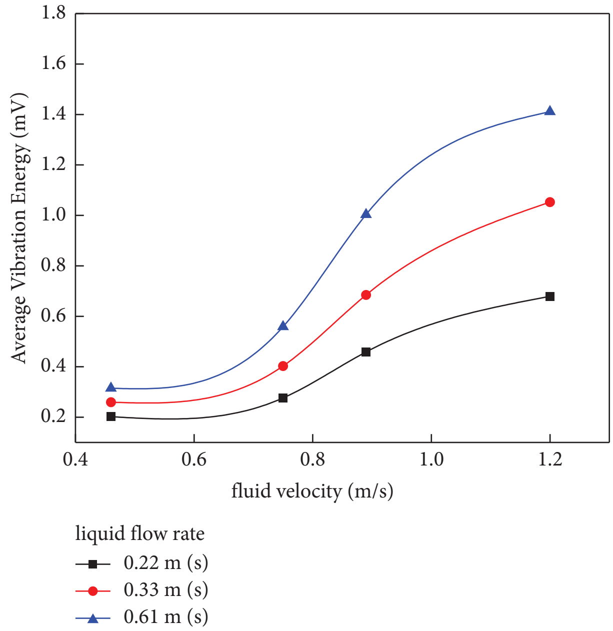

Figure 10: Energy analysis of signals excited by liquid particles impacting on the pipe wall under different liquid flow rates and flow velocities.

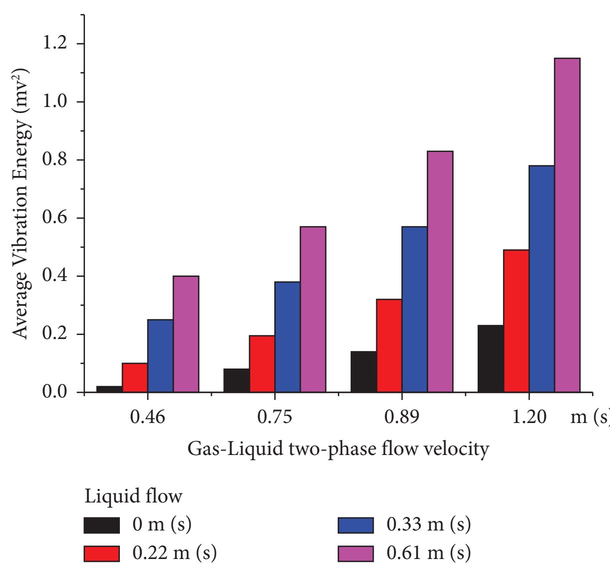

Figure 11: The distribution of vibration energy excited by gas-liquid two-phase flow impacting on the elbow pipe wall under different liquid flow rates and flow velocities.

Table 2: The list of coefficient values in formula (9).

Corner mark	b	Square value of correlation coefficient
0	0.44483	0.99
1	−2.0011	0.99
2	2.85479	0.99
3	−1.11366	0.99

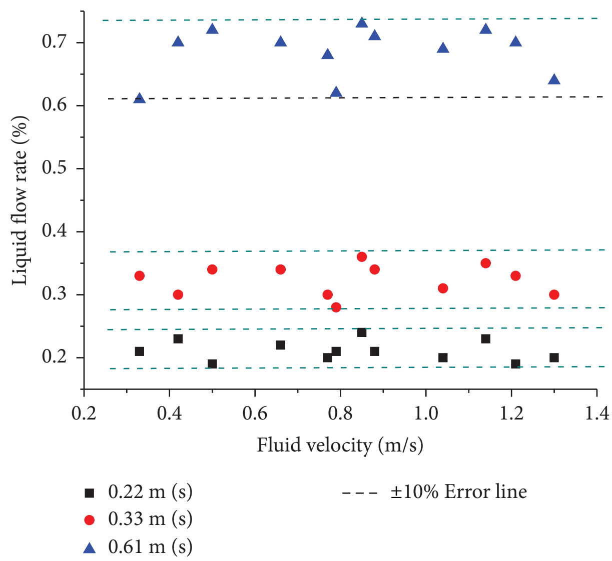

FIGURE 12: Collection of liquid flow rates at different fluid velocities.

above and below the theoretical value. The resulting analysis in the figure shows that the calculation method can weaken the influence of the calculation results under the conditions of different liquid flow rates and different flow velocities. Therefore, the vibration signal processing method based on STFT time-frequency analysis can realize the quantitative and accurate detection of liquid flow rate in gas-liquid two-phase flow.

The use range of the calculation model is as follows: the condition is controlled at the flow rate v: 0.4 m/s–1.2 m/s. The liquid flow rate is calculated in the range of 0.2–0.6 m/s.

6. Conclusion

In this paper, the liquid flow characteristics in gas-liquid two-phase flow are detected and analyzed by the time-frequency analysis method based on the vibration signal characteristic analysis. By analyzing the time-frequency characteristics of the vibration signals excited by the airflow impacting on the pipe wall at different flow velocities and the gas-liquid two-phase flow impacting on the pipe wall under different liquid contents, it is shown that the amplitude of the vibration signal excited by the airflow impacting on the pipe wall is the smallest and the signal is stable in the frequency band of 6.5–15 Hz. Therefore, this frequency band is identified as the characteristic frequency band of the vibration signals excited by the liquid particle impacting on the pipe wall. At the same time, with the increase in liquid flow rate, the signal's amplitude in the characteristic frequency band is positively correlated with it. Therefore, the validity of 6.5–15 Hz frequency band as the characteristic frequency band of liquid flow is verified again, and the mathematical model of the relationship between liquid holdup and vibration energy is constructed. The research method has laid a good research foundation for the subsequent detection of each phase in complex gas-liquid-solidthree-phase flow and gas-solid two-phase flow.

Data Availability

The data used to support the findings of this study are available from the corresponding author upon request.

Conflicts of Interest

The authors declare that there are no conflicts of interest regarding the publication of this paper.

Acknowledgments

This research was sponsored by the Education Department of Hubei Province; Wuhan University of Technology; Jingzhou Municipal People's Government; Optical Fiber Sensing Sub_Marine Cable System for safety monitoring of deep-sea riser, Grant no. SKJC-2020-01-016; Sanya Yazhouwan Science and Technology City Project, Grant no. SKJC-KJ-2019KY02; Key Project of China Petrochemical Company: Research on Distributed Optical Fiber Flow Monitoring and Interpretation Technology, Grant no. P21052; Science and Technology Research Project of Education Department of Hubei Province, Guiding Project, Grant no. B2021041; Humanities and Social Sciences Research Project of Education Department of Hubei Province, Grant no. 20D038; 2021 Science and Technology Research Project of Jing Zhou City, Grant no. 2021CC28-16; Industry-University Cooperation Collaborative Education Project of Ministry of Education in 2020, Grant no. 202002077032; and Industry-University Cooperation Collaborative Education Project of Ministry of Education in 2021, Grant no. 202102077032. These supports are gratefully acknowledged.

References

[1] N. Zhao, P. P. Wang, and S. N. Guo, "Interfacial disturbance wave velocity of gas-liquid two-phase annular flow in vertical pipe," *Cambridge Assessment International Education Journal*, vol. 69, no. 7, pp. 2926–2934, 2018.

[2] X. D. Liu, Q. Sun, and L. Y. Wu, "Progress in numerical simulation of multiphase flow in microchannels," *Chemical Industry and Engineering Progress*, vol. 35, no. S2, pp. 32–40, 2016.

[3] C. Shen, Q. B. Pei, and B. T. Liu, "The Evaluation of Uncertainty of Flow Totalizer Standard Facility," *Acta Metrologica Sinica*, vol. 38, no. 3, pp. 333–335, 2017.

[4] C. Tan and F. Dong, "Parameters measurement for multiphase flow process," *Acta Automatica Sinica*, vol. 39, no. 11, p. 1923, 2013.

[5] S. Yino, "Research advances of PIV in GasLiquid phase flow," *Petroleum Engineer*, vol. 25, no. 2, pp. 1–3, 2006.

[6] H. T. Situr and J. Brownr, "Flow regime transition criteria for two-phase flow at reduced gravity conditions," *International Journal of Multiphase Flow*, vol. 37, pp. 1165–1177, 2011.

[7] K. Z. Wang and L. Jia, "Vibration signal characteristics analysis for sand detection in gas-sand two-phase flow," *Journal of Tianjin University*, vol. 51, no. 11, pp. 153–158, 2018.

[8] Z. J. Fang, *In-tube Separation and Flow Rate Measurement of Gas-Liquid Two Phase Flow*, China University of Petroleum, Beijing, China, 2020.

[9] C. Y. Wang, *Study on Flow Measurement Technology of Multiphase Flow Frequency Difference Method*, Xi'an Shiyou University, Xi'an, China, 2021.

[10] J. W. Murdock, "Two-phase flow measurements with orifices," *Journal of Basic Engineering*, vol. 84, no. 4, pp. 419–433, 1962.

[11] D. Chisholm, "Void fraction during two-phase flow," *Journal of Mechanical Engineering Science*, vol. 15, no. 3, pp. 234-235, 1973.

[12] Y. Xu, "Research on two-phase flow model for wet gas based on Venturi flow sensor," *Transducer and Microsystem Technologies*, vol. 35, no. 5, pp. 4–9, 2016.

[13] M. M. Li, *Study on the New Phase Volume Fractiondetection Device of Gas-Liquid Two-phase flow*, Hebei University, Hebei Baoding, China, 2016.

[14] L. D. Fang, S. C. Wang, and P. P. Wang, "Phase volume fraction measurement of gas-liquid two-phase flow based on near-infrared surface source sensor," *Actarologica Sinica*, vol. 40, no. 6, pp. 7–11, 2019.

[15] Y. J. Liang, *Study on Phase Volume Fractiondetection of Gas-Liquid Two-phase Flowbased on Near-Infrared Absorbance feature*, Hebei University, Hebei Baoding, China, 2016.

[16] X. Zhang, M. qin, and S. Sheng-kui, "The ultrasonic mass flow measurement method of light fuel based on the artificial neural network model," *Acta Metrologica Sinica*, vol. 38, no. 2, pp. 205–210, 2017.

[17] L. Hou, Y. Yang, and X. Hu, "Study on particle size distribution in gas-solid fluidized bed by acoustic emission measurement," *Petrochemical Technology*, vol. 32, no. S1, pp. 893–895, 2003.

[18] F. Ong, M. Uecker, U. Tariq et al., "Robust 4D flow denoising using divergence-free wavelet transform: 4D Flow Denoising with DFW Transform," *Magnetic Resonance in Medicine*, vol. 73, no. 2, pp. 828–842, 2015.

[19] B. H. Aghdam, M. Vahdati, and M. H. Sadeghi, "Vibration-based estimation of tool major flank wear in a turning process using ARMA models," *The International Journal of Advanced Manufacturing Technology*, vol. 76, no. 9-12, pp. 1631–1642, 2015.

[20] W. Y. Liu, "Auto term window method and its parameter selection," *Measurement*, vol. 46, no. 9, pp. 3113–3118, 2013.

[21] K. Wang, G. Liu, J. Wu et al., "Acoustic sensor approaches for sand detection in sand–water two-phase flows," *Powder Technology*, vol. 320, pp. 739–747, 2017.

[22] Z. Wu, F. L. Yi-Li, M. Long-Tao, and L. Ji-Guo, "Grid harmonic detection method based onCombination of wavelet packet transform and FFT [J]," *Power System and Automation*, vol. 41, no. 2, pp. 44–56, 2019.

[23] Q. Zhou and C. Han, "Analyzing for power system harmonics with time-varying characteristics based on time-frequency analysis method [J]," *Journal of Shan-xi University of Science and Technology*, vol. 36, no. 4, pp. 147–154, 2018.

[24] L. I. Yichen, G. Liu, Z. Jia et al., "Experimental investigations of offshore sand production monitoring based on the analysis of vibration in response to weak shocks," *Geofluids*, vol. 2021, Article ID 9953498, 17 pages, 2021.

[25] Z. Peng, R._Q. Liao, G._Q. Wang, and X._R. He, "Experimental and numerical simulation study on two phase flow in VerticalPipe at high gas-liquid flow rates," *Oil-gasfield Surface Engineering*, no. 3, pp. 41–44, 2016.

[26] F. Liang, J. Zhao, M. Jia, Q. Li, and N. Li, "Gas-liquid Plug Flow Liquid Holdup Measurement Using Semantic Segmentation," *Oil and Gas Storage and Transportation*, 2021.

[27] H._J. Wang, "Digital FIR filter design based on window function segmentation," *Digital FIR Filter Design Based on Window Function Segmentation*, vol. 37, no. 08, pp. 169–171, 2017.